


 Cite this: *RSC Adv.*, 2024, **14**, 33649

## Production, characterization and environmental remediation application of emerging phosphorus-rich biochar/hydrochar: a comprehensive review†

 Qilong Ge, <sup>\*a</sup> ChunJuan Dong,<sup>a</sup> GuoYing Wang,<sup>b</sup> Jing Zhang<sup>a</sup> and Rui Hou<sup>c</sup>

Owing to the high carbon and phosphorus contents, large specific surface area and slow P release capacity of P-rich biochar/hydrochar (CHAR), its application in aquatic (or soil) environments and positive effects on heavy metal (HM) adsorption (or immobilization) have drawn global attention. To provide an overall picture of P-rich CHAR, this review includes a systematic analysis of the current knowledge on the preparation methods, characterization techniques, influencing factors and environmental applications of P-rich CHAR reported in the last ten years. The key findings and recommendations from this review are as follows: (1) there is still a knowledge gap concerning the regulatory mechanism of the key active components of P-rich CHAR at the molecular level. The dominant factors influencing these active components should be elucidated. (2) P-rich CHAR has a high capacity to immobilize most HMs (e.g., Cd, Cu, and Pb). However, it performs poorly with several HMs (e.g., As). Future studies should focus on the interactions between P-rich CHAR and HMs found in soil/water. (3) To meet the long-term requirements for plant growth, more attention should be given to improving the slow-release capacity and utilization efficiency of available P. (4) There is a potential risk of P loss (or eutrophication) due to rainfall and runoff, although P-rich CHAR exhibits excellent performance in terms of HM immobilization and carbon retention. Several reasonable suggestions are provided to solve these problems. In summary, P-rich CHAR has promising prospects in environmental remediation if these shortcomings are overcome.

Received 6th May 2024

Accepted 10th October 2024

DOI: 10.1039/d4ra03333g

[rsc.li/rsc-advances](http://rsc.li/rsc-advances)

### 1. Introduction

As a carbon material derived from biomass, biochar/hydrochar (CHAR) has been extensively applied in soil remediation and wastewater treatment and as agricultural fertilizer.<sup>1–3</sup> Owing to their high carbon content and low cost, these materials have garnered significant attention over the past decade. The increasing number of published studies (Fig. 1(a) and (b)) underscores the rising prominence of CHAR as a research focal point. The data presented in Fig. 1 were extracted from the Elsevier Science Direct database, with only English language publications included in the analysis. The search was conducted using the keywords “biochar” and “hydrochar”. However, owing to the limited number of adsorption sites and the suboptimal adsorption performance of unmodified CHAR,

many researchers have increasingly focused on enhancing its properties through various modification techniques.<sup>4–5</sup>

P-rich CHAR refers to biochar or hydrochar with a high phosphorus (P) content, typically ranging from 1% to 8%, which is significantly higher than the P content in unmodified CHAR (commonly less than 0.5%).<sup>6–8</sup> Studies have shown that the presence of phosphorus atoms in CHAR plays a crucial role in altering its physicochemical properties.<sup>9–23</sup> Owing to its large covalent radius, low electronegativity and specific valence electron structure, phosphorus modifies the surface functional groups of CHAR, increasing the activity of this carbon material. Consequently, P-rich CHAR demonstrates excellent performance in the immobilization of heavy metals (HMs) present in the soil, HM adsorption in aqueous solutions, and as a slow-release phosphorus fertilizer.<sup>5–7</sup> For instance, Zhao *et al.*,<sup>14</sup> found that  $K_3PO_4$ -modified biochar significantly improved the immobilization capacity for Cu and Cd in soil. Similarly, Gao *et al.*,<sup>11</sup> reported that biochar modified with  $Ca(H_2PO_4)_2H_2O$  and  $KH_2PO_4$  enhances  $Pb^{2+}$  removal from wastewater. Recently, biochar-based slow-release P fertilizers with high water retention and a substantial amount of Fe/Al-bound P have been developed to increase the efficiency of P utilization in the soil.<sup>12</sup> Additionally, most P-containing modification agents are non-toxic and easily washed off with water, making P-rich CHAR a reliable and environmentally friendly choice.

<sup>a</sup>Department of Architecture and Environmental Engineering, Taiyuan University, Taiyuan 030032, China. E-mail: Geqilongde@163.com

<sup>b</sup>College of Environmental Science and Engineering, Taiyuan University of Technology, Taiyuan 030024, China

<sup>c</sup>South China Sea Institute of Oceanology, Chinese Academy of Sciences, Guangzhou 510301, China

† Electronic supplementary information (ESI) available. See DOI: <https://doi.org/10.1039/d4ra03333g>



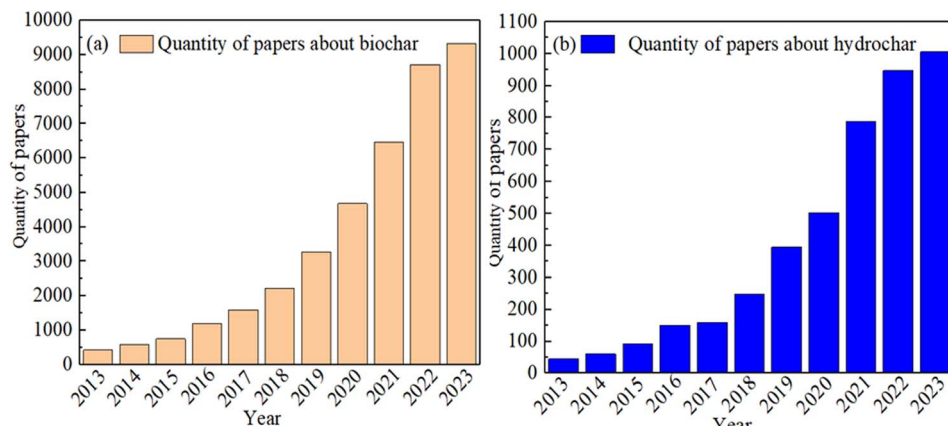


Fig. 1 Number of papers about (a) biochar and (b) hydrochar published in the last ten years.

However, to date, there has been no comprehensive review on the production, characterization and environmental application of P-rich CHAR. Over the past ten years, extensive research has been conducted worldwide on P-rich CHAR, providing a valuable foundation for a review that offers a deeper understanding of its preparation and potential use in environmental remediation. Although P-rich CHAR demonstrates significant promise in environmental applications, several potential risks must be considered. For instance, to achieve optimal HM immobilization in soils, the applied content of P-rich CHAR typically exceeds 3%, which can lead to the loss of available P.<sup>13,14,16,24</sup> Another limitation is that, even with the addition of P-rich CHAR, the slow release rate of P available in the soil often surpasses the plant uptake rate.<sup>25</sup> These drawbacks restrict the broader application of P-rich CHAR. Furthermore, the mechanisms underlying the preparation of P-rich CHAR and the regulation of the key active components, such as P/O-containing functional groups, and the Fe/Al/Ca-bound P content require further investigation. To address these knowledge gaps, future research directions and guidance for devising solutions are needed.

So far, most reviews have focused predominantly on general information on CHAR, with only a few offering a comprehensive overview of P-rich CHAR. In light of this, the overall goal of this systematic review is to provide a comprehensive perspective on P-rich CHAR, with valuable insights into the potential of P-rich CHAR as an environmental remediation agent. The specific objectives of this review are: (1) to elucidate the synthetic methods and the factors influencing the preparation of P-rich CHAR, (2) to present the fundamental properties and characterization techniques of P-rich CHAR, (3) summarize their environmental applications, (4) assess the potential environmental risks posed by P-rich CHAR, and (5) provide recommendations for their future utilization.

## 2. Methodology

This review was conducted in accordance with the standards set by the Preferred Reporting Items for Systematic Review and

Meta-Analysis Statement.<sup>26</sup> Literature searches for this review were performed from 2013 to 2023 *via* the Web of Science and Google Scholar. The following four keywords were used for the literature search: P-rich biochar, P-modified biochar, P-rich hydrochar, and P-modified hydrochar. The retrieved articles were meticulously evaluated, and only peer-reviewed studies pertinent to the preparation, characterization and environmental application of P-rich CHAR were selected. Finally, from the 81 retrieved publications, a total of 41 publications were selected (Table S1†). The eligibility criteria for the inclusion of articles were as follows: (1) production: preparation (or synthesis) of P-rich CHAR; (2) characterization: properties and associated testing methods of P-rich CHAR; and (3) environmental application: HM immobilization in the soil, carbon retention, release of available P, and HM adsorption in water. Articles were excluded based on the following criteria: (1) production: preparation (or synthesis) of CHAR; (2) characterization: properties and corresponding testing methods of CHAR; (3) environmental application: supercapacitor and CO<sub>2</sub> adsorption.

## 3. Preparation of P-rich CHAR

P-rich CHAR materials produced by various methods exhibit distinct physicochemical properties. Fig. 2 summarizes three widely employed techniques, namely co-pyrolysis, pyrolysis impregnation and hydrothermal carbonization (HTC). The P-rich carbon materials generated *via* co-pyrolysis or pyrolysis impregnation are commonly referred to as P-rich biochar, whereas those produced through the HTC method are designated as P-rich hydrochar.<sup>27</sup>

### 3.1 Co-pyrolysis method

The co-pyrolysis method involves the pyrolysis of a mixture of biomass feedstock and P-containing compounds (*i.e.* K<sub>3</sub>PO<sub>4</sub>, KH<sub>2</sub>PO<sub>4</sub>) at temperatures ranging from 450 °C to 700 °C under anaerobic conditions.<sup>28</sup> Depending on the residence time, co-pyrolysis can be classified into three categories: fast, intermediate, and slow pyrolysis.<sup>3</sup> Fast pyrolysis involves introducing



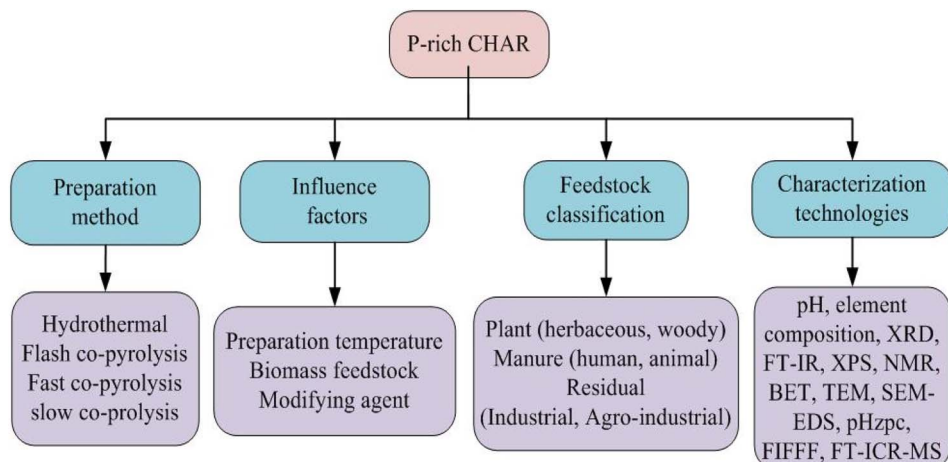


Fig. 2 Preparation methods, feedstock classification, characterization techniques and factors influencing the preparation of P-rich CHAR.

a mixture of feedstock and P-containing compounds into the reaction vessel at the designated temperature, and the reaction time is typically several seconds. This method is frequently employed to produce bio-oil.<sup>29</sup> In contrast, intermediate and slow pyrolysis involve longer residence times, ranging from several minutes to a few hours. Compared with fast pyrolysis, slow pyrolysis is generally preferred because of its higher yield and increased carbon content.<sup>30</sup>

### 3.2 Pyrolysis impregnation method

The pyrolysis impregnation method involves the initial preparation of pyrolytic products, which are subsequently combined with P-containing compounds. Wang *et al.*,<sup>31</sup> and Ng *et al.*,<sup>32</sup> produced peanut shell biochar at 500 °C and immersed it in a 10 g L<sup>-1</sup> K<sub>3</sub>PO<sub>4</sub> solution to enhance P loading on the biochar surface at room temperature. In comparison, the specific surface area (SSA) of the P-rich biochar generated *via* the co-pyrolysis method is larger, resulting in a greater number of P-containing functional groups on its surface. Furthermore, a more diverse array of P compositions can be observed. These P compositions are typically categorized into dissolved and exchangeable P, Fe/Al-bound P, Ca-bound P and residual P.

### 3.3 Hydrothermal carbonization (HTC) method

HTC refers to the carbonization of a two-phase mixture comprising a P-containing solution and fresh feedstock, without the need for drying pretreatment.<sup>33</sup> The mixture is placed in a reactor, and the temperature and (or) pressure are subsequently elevated. Daer *et al.*,<sup>34</sup> demonstrated HTC by combining corn straw and phosphorus rock in a reactor, producing P-rich hydrochar at a temperature of 220 °C with a residence time of 240 min. This energy-saving method operates in the temperature range of 120 °C to 250 °C, indicating that the reaction conditions of HTC are milder than those of co-pyrolysis. However, two significant drawbacks hinder the wide acceptance of the HTC method: the need for high pressure and the generation of wastewater during the process. The

wastewater produced is often contaminated with toxic pollutants and therefore requires treatment to comply with environmental requirements.<sup>35</sup>

## 4. Primary factors influencing the preparation of P-rich CHAR

### 4.1 Temperature

The preparation of P-rich biochar can be divided into three stages on the basis of comparative thermo-gravimetric and differential thermal analyses of pristine and P-rich biochar.<sup>36–38</sup> In the first stage (25–200 °C), an initial mass reduction occurs likely due to the evaporation of moisture and the release of a small amount of volatiles. During this phase, the internal pore structure of P-rich biochar undergoes realignment as a result of moisture evaporation and the chemical bonds break. In the second stage (200–500 °C), a significant mass loss is observed because of the polymerization of organic compounds, such as hemicellulose and cellulose. The third stage ( $\geq 500$  °C) involves the degradation of organic matter with stronger chemical bonds, leading to gradual weight reduction. The elemental compositions (*i.e.* C, O, H, N, and P) of the P-rich samples vary with changes in the pyrolysis temperature. Studies indicate that as the temperature increases, the P and C contents initially rise and then decrease. Generally, the H/C ratio serves as an indicator of the degree of carbonization; a decrease in the H/C ratio corresponds with increased aromaticity.<sup>39</sup> Similarly, lower (O + N)/C and O/C ratios reflect reduced polarity and greater oxygen removal. These two ratios reflect the stability of the P-rich biochar.<sup>10</sup> P-rich biochar obtained at relatively high pyrolysis temperatures predominantly contains aromatic compounds and has reduced polarity.<sup>35</sup> Moreover, the surface area and concentration of the P-containing functional groups increase with increasing pyrolysis temperatures. Thus, the physical and chemical adsorption capacities of the P-rich biochars improve, enabling the adsorption of most pollutants. Nevertheless, Zhang *et al.*,<sup>40</sup> found that an excessively high pyrolysis temperature results in the collapse of the tunnel structures in P-rich



biochar. The specific surface area of the P-rich biochar decreases, and the pollutant adsorption capacity decreases. Similarly, Peng *et al.*<sup>41</sup> reported that a relatively high pyrolysis temperature reduces the diversity of functional groups, consequently diminishing the adsorption of pollutants on the P-rich biochar.

In contrast, the temperature required for the preparation of P-rich hydrochar is relatively mild. The mechanism primarily involves the thermochemical conversion of the biomass feedstock under subcritical water conditions. During this process, the biomass undergoes a series of complex chemical reactions, including dehydration, decarboxylation and polycondensation reactions.<sup>2</sup> Generally, in a specific temperature range, a higher preparation temperature results in increased surface area, greater abundance of surface functional groups, and a greater degree of carbonization in the resultant P-rich hydrochar.<sup>42</sup> Studies have confirmed the presence of numerous functional groups, such as hydroxyl [ $-\text{OH}$  ( $3450 \text{ cm}^{-1}$ )], carboxyl [ $-\text{COOH}$  ( $1701 \text{ cm}^{-1}$ )], methylene [ $-\text{CH}_2$  ( $2920 \text{ cm}^{-1}$ )], and P-containing groups [ $\text{P}=\text{O}$  or  $\text{P}-\text{O}-\text{C}$  ( $1220 \text{ cm}^{-1}$ )] on the surface of P-rich hydrochar. The Fourier transform infrared (FT-IR) spectra of  $\text{H}_3\text{PO}_4$ -modified hydrochar derived from cauliflower leaves and banana peels prepared at different temperatures are shown in Fig. 3.<sup>43</sup> In the given range of hydrothermal temperatures, the concentration of the O-containing and P-containing functional groups increases with rising temperature, probably because the catalytic chemical degradation reaction is controlled by the number of protons.<sup>44</sup> Additionally, the formation of these functional groups is enhanced by phosphate radicals.<sup>22</sup> However, at higher temperatures (*i.e.*  $240^\circ\text{C}$ ), the number of functional groups decreases significantly because of excessive dehydration induced by proton activity at elevated temperatures.<sup>45</sup> Furthermore, higher preparation temperatures typically lead to an increase in the inorganic elemental content (*i.e.* Ca, K, P) and minerals of P-rich hydrochar as a result of the volatilization of more organic compounds.<sup>46</sup>

In summary, the heating temperature plays a critical role in determining the surface pore structure, surface functional

groups, and elemental content of P-rich CHAR. Maintaining the optimal temperature during the preparation process is essential for achieving P-rich CHAR with unique physical and chemical properties. These fundamental characteristics directly influence its effectiveness in environmental applications.

## 4.2 Feedstock

As presented in Table S1,<sup>†</sup> the feedstock sources of P-rich biochar are diverse and primarily consist of low-cost organic waste, including agricultural waste (*i.e.* corn straw, cotton straw, and wheat straw), garden waste (*i.e.* deadwood and rotten leaves), municipal waste (*i.e.* sludge), and animal waste.<sup>47</sup> These materials are rich in essential nutrients (*i.e.* C and N), as well as cellulose, hemicelluloses, and lignin, which make them highly suitable for the preparation of P-rich biochar. Fig. 2 illustrates the classification of biomass feedstocks. Based on initial moisture content, the raw materials can be categorized into dry and wet biomass types. According to the growing conditions, the feedstock is derived primarily from either aquatic biomass or terrestrial biomass.<sup>48</sup> In addition, according to the source, the feedstock can be classified into plant, manure, and residual.<sup>46</sup> P-rich biochar can be prepared from a wide range of carbonaceous materials, such as plant leaves, wood, manure, agricultural residuals, and food waste. Studies have shown that P-rich biochars derived from different feedstock sources present significant variation in their structural and functional properties.<sup>49</sup> Given that lignin tends to form P-rich biochar more readily during carbonization, biomasses with higher cellulose content, such as plant matter, typically yield greater quantities of P-rich biochar than materials with lower cellulose content.<sup>50</sup>

The feedstock sources of P-rich hydrochar are similarly diverse (Table S2<sup>†</sup>). Fig. 4 depicts a Van Krevelen diagram plotted based on data from Table S2<sup>†</sup> illustrating the H/C and O/C atomic ratios. It visually demonstrates the enhanced properties of the P-rich hydrochars compared to the original raw biomass. The moisture content in the feedstock plays a significant role in determining the preparation conditions of P-rich CHAR. Fast pyrolysis always requires dry biomass, as

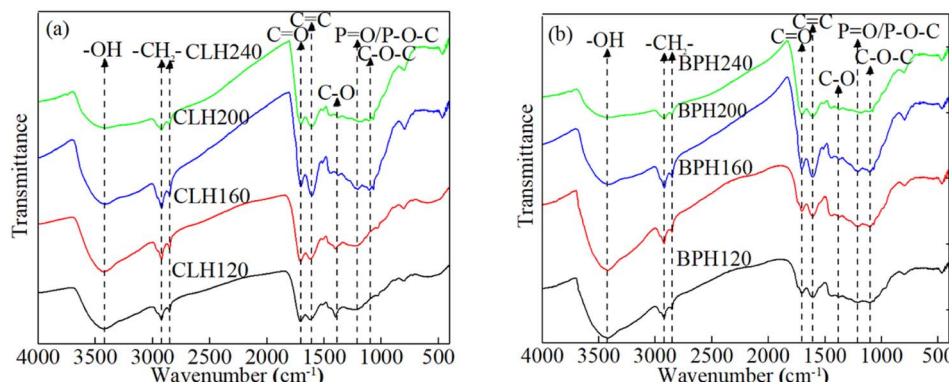


Fig. 3 FT-IR spectra of  $\text{H}_3\text{PO}_4$ -modified hydrochar derived from (a) cauliflower leaves and (b) banana peels at different hydrothermal temperatures.<sup>43</sup> Note: The modified hydrochars prepared from cauliflower leaves and banana peels are labeled CLH and BPH, respectively. CLH and BPH prepared at  $120^\circ\text{C}$ ,  $160^\circ\text{C}$ ,  $200^\circ\text{C}$  and  $240^\circ\text{C}$  are marked as CLH120, BPH120, CLH160, BPH160, CLH200, BPH200, CLH240, and BPH240, respectively.



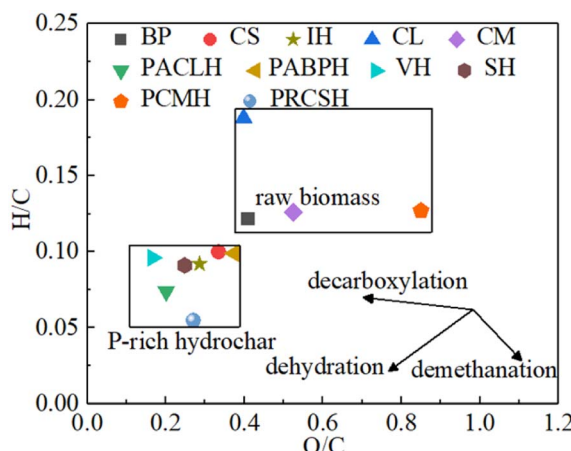


Fig. 4 Van Krevelen diagram for P-rich hydrochars derived from different raw materials (BP: banana peel; CS: corn straw; IH: indica hydrochar; CM: cow manure; PACLH: phosphoric-acid-modified cauliflower leaves hydrochar; PABPH: phosphoric-acid-modified banana peels hydrochar; VH: verticillata hydrochar, SH: spicatum hydrochar; PCMH: potassium-modified cow manure hydrochar; PRCSH: phosphate-rock-modified corn straw hydrochar).

water evaporation can hinder the rise in temperature. In contrast, slow pyrolysis is more tolerant of moisture. Wet biomass feedstocks, such as algae and sludge, are suitable for the preparation of P-rich hydrochar through HTC.<sup>35</sup> Moreover, in the production of P-rich hydrochar, an additional separation step is often necessary to isolate the hydrochar from the final solid–liquid mixture.<sup>35</sup>

Moreover, both preparation and feedstock costs are also critical factors. From an economic standpoint, P-rich CHAR can be more efficiently synthesized using feedstocks that are already rich in P. Researchers often employ the index of the cost/benefit ratio to measure the sustainability and economic effectiveness of this biotechnology.<sup>51</sup> For example, because algae are easy to acquire and rich in phosphorus, they are widely used as cost-effective material for P-rich CHAR production, particularly, when they are harvested from eutrophic water bodies. The P-rich CHAR derived from algae has been shown to improve soil properties and immobilize HMs in the soil more effectively and at a lower cost compared to biochar produced from other biomass feedstocks.<sup>52,53</sup>

### 4.3 Modifying agents

Phosphate and phosphate minerals (*i.e.*  $\text{KH}_2\text{PO}_4$ ,  $\text{K}_3\text{PO}_4$ ,  $\text{Ca}(\text{H}_2\text{PO}_4)_2$  and P fertilizer) are commonly utilized in the production of P-rich biochar. The available form of P significantly influences the mechanisms underlying pollutant removal by P-rich biochar. Wang *et al.*,<sup>54</sup> investigated the different P forms present in P-modified biochar derived from apple tree branches combined with  $\text{KH}_2\text{PO}_4$ ,  $\text{K}_2\text{HPO}_4 \cdot 3\text{H}_2\text{O}$ , and  $\text{K}_3\text{PO}_4 \cdot 3\text{H}_2\text{O}$ , respectively. Orthophosphates (24.8%), pyrophosphates (73.7%), and metaphosphates (1.49%) were detected in the  $\text{KH}_2\text{PO}_4$ -modified biochar (BC-1). In contrast, orthophosphates (47.4%) and pyrophosphates (52.6%) were observed in the  $\text{K}_2\text{HPO}_4 \cdot 3\text{H}_2\text{O}$ -modified biochar (BC-2). More

orthophosphate (86.2%) and less pyrophosphate (13.8%) were found in the  $\text{K}_3\text{PO}_4 \cdot 3\text{H}_2\text{O}$ -modified biochar (BC-3). The maximum adsorption capacity for  $\text{Cd}^{2+}$  followed the order BC-3 > BC-2 > BC-1. These results indicate that orthophosphate promotes  $\text{Cd}^{2+}$  adsorption through the formation of Cd-P precipitates.

P-Containing additives can uniformly infiltrate cellulose and lignin. Under high temperatures, water vapor is produced by a catalytic dehydration reaction between cellulose/lignin and P-containing additives. Subsequently, many pores are created.<sup>9,10</sup> Therefore, infiltration of P-containing additives into the internal pores and channels of biochar, along with effective dispersion, is typically observed. After washing, the developed pore structure can be visualized. However, certain P-containing additives, such as  $(\text{NH}_4)_3\text{PO}_4$ , may lead to the collapse of the pore structure of P-rich biochar. This deterioration is attributed to the release of ammonia gas during pyrolysis, which can adversely affect the formation of micropore and mesopore structures.

For the modification of P-rich hydrochar, phosphoric acid ( $\text{H}_3\text{PO}_4$ ) and soluble phosphates are commonly employed.  $\text{H}_3\text{PO}_4$  is a typical modifying agent. Zhou *et al.*,<sup>21</sup> found that when the concentration of  $\text{H}_3\text{PO}_4$  is greater than 30 wt% during HTC, the decomposition of hemicelluloses and cellulose overlaps, leading to a high yield of P-rich hydrochar. The multi-functional roles of  $\text{H}_3\text{PO}_4$  are as follows: (1)  $\text{H}_3\text{PO}_4$  facilitates the dehydration of biomass and reduces the temperature required for biomass decomposition during carbonization; (2)  $\text{H}_3\text{PO}_4$  enhances carbon retention in the biomass; (3)  $\text{H}_3\text{PO}_4$  introduces P-containing substances and groups into the hydrochar, which is conducive to immobilizing HMs in the soil and providing nutrients; and (4)  $\text{H}_3\text{PO}_4$  reduces the temperature required for decomposition of biomass fibrocytes.<sup>22</sup>

In addition, the addition of P-containing additives during HTC often results in an increase in the number of P-containing and O-containing functional groups. These groups remain fixed on the surface and internal pore walls of P-rich hydrochar through catalytic dehydration and cross-linking reactions.<sup>11,12</sup> Consequently, the size of most pores is reduced, leading to a transformation from mesopores to micropores. The Van Krevelen diagram (Fig. 4), which illustrates the H/C and O/C atomic ratios, further elucidates the role of P-containing additives in the HTC process. Both the O/C and H/C ratios of P-rich hydrochars tend to shift downward and to the left, reflecting an enhancement in aromatization during HTC. These findings suggest that P-containing additives facilitate deoxygenation and dehydrogenation reactions during HTC.

## 5. Characterization techniques for P-rich CHAR

Fig. 2 also presents the techniques used for P-rich CHAR characterization. The pH value of P-rich CHARs can be identified by a pH meter after stirring the slurry, in which the ratio of P-rich CHAR to water is 1 : 2.5 or 1 : 10 (w/v).<sup>55,56</sup> Most P-rich biochars prepared *via* co-pyrolysis are weakly alkaline (approximately 7–



10) likely due to the formation of mineral substances, such as carbonates.<sup>57</sup> However, P-rich hydrochar produced *via* HTC is acidic even without the addition of acid additives. The reason is the acceleration of dehydration and degradation of polysaccharides in water during the HTC process. Moreover, many acidic functional groups and low molecular acids are formed and remain attached to the surface of the P-rich hydrochar.<sup>21</sup>

Because of the importance of pH, the identification of the point of zero charge ( $pH_{pzc}$ ) of P-rich CHAR is also important. Two methods are usually used to measure this index of P-rich CHAR: (1) the zeta potential of the P-rich CHAR is detected at different pH values. The measured data are fitted linearly to identify the pH at which the zeta potential is zero;<sup>58</sup> (2) the P-rich CHAR is added to NaCl solutions at different pH values and allowed to react for some time. The difference between the pH values of the initial and final solutions represents the  $pH_{pzc}$ .<sup>59</sup> Most P-rich CHARs are negatively charged, and the surface charge and  $pH_{pzc}$  are often changed by P compound modifications.<sup>16,18,60</sup> Chen *et al.*<sup>60</sup> prepared a P-rich biochar from chicken feathers *via* phosphoric acid impregnation combined with the co-pyrolysis method. The  $pH_{pzc}$  of the  $H_3PO_4$ -modified biochar was 3.53, which is lower than that (5.53) of the pristine biochar. Because of this, the cadmium and lead adsorption capacity of the  $H_3PO_4$ -modified biochar was improved. Ge *et al.*<sup>8</sup> found similar results by preparing a P-rich hydrochar derived from cauliflower leaves *via*  $H_3PO_4$  impregnation combined with the HTC method. This wide range of  $pH_{pzc}$  values can be explained by the use of different raw materials and preparation methods, and consequently, the distinct physico-chemical properties of P-rich CHAR.

They are primarily composed of C, H, O, P and N. The range of C content is usually 38–80%. Most of the organic matter in P-rich CHAR includes alkyl and aromatic compounds.<sup>35</sup> Besides, the P content in P-rich CHAR is much greater than that in pristine CHAR.<sup>8</sup> Other nutrients, such as Si, Na and Mg, are often detected in P-rich CHAR.<sup>27</sup> The elemental content can be identified using an elemental analyzer. The elemental composition also differs from the raw materials from which the P-rich CHARs are prepared. In addition, the preparation conditions (*i.e.* temperature, P-containing additive, *etc.*) of P-rich CHAR also affect the elemental content.<sup>6</sup>

The surface functional groups of P-rich CHAR critically influence its soil remediation and pollutant adsorption capacity. Therefore, further investigation of the adsorption and remediation mechanisms of these groups will help improve the surface functionalization of P-rich CHAR. FT-IR spectroscopy and X-ray photoelectron spectroscopy (XPS) are usually used. As a qualitative analysis method, FT-IR has been widely used to study the surface functional groups of P-rich CHAR. According to the literature, the typical functional groups found in P-rich CHAR are as follows:  $-OH$  (around  $3400\text{ cm}^{-1}$ ),  $-CH_2-$  ( $2920\text{ cm}^{-1}$ ),  $-COOH$  ( $1720\text{ cm}^{-1}$ ),  $C=O$  ( $1600\text{ cm}^{-1}$ ),  $P=O/P-O-C$  ( $1220\text{ cm}^{-1}$ ), and  $P-O-P/P^+-O^-$  ( $1070\text{ cm}^{-1}$ ).<sup>41,61</sup> Therefore, on the basis of the changes in these peaks, the functional groups on the P-rich CHAR found before and after modifications can be determined. In addition, FT-IR can reveal the mechanism of adsorption in solutions and the extent of soil

remediation after the application of the P-rich CHAR.<sup>62</sup> Furthermore, the peaks of P-containing functional groups, such as  $P=O/P-O-C$  ( $1220\text{ cm}^{-1}$ ),  $PO$  ( $1080\text{ cm}^{-1}$ ), and  $P-O-P/P^+-O^-$  ( $1070\text{ cm}^{-1}$ ), indirectly verify the successful preparation of P-rich CHAR.<sup>41,63</sup> Most of these functional groups are attributed to the fixation of enormous amounts of P on the surface of the P-rich CHAR. However, excessively high temperatures promote the hydrophobicity of P-rich CHAR, leading to a rapid decrease in the number of polar functional groups.<sup>64</sup> The elements present on the surface of P-rich CHAR and their valence states can be measured before and after modification by XPS. Because different elements have different values of binding energy for the same inner shell electron, the photoelectron peak of the given inner shell electron shifts according to the molecules in which the element is located. For instance, in  $K_3PO_4$ -modified wood biochar and rice husk biochar ],<sup>10</sup> high peak energies of P 2p at  $133.5 \pm 0.1\text{ eV}$  and  $134.5 \pm 0.1\text{ eV}$  were observed compared with the pristine biochar, respectively. These newly formed peaks indicate the appearance of  $P-O$  and  $P=O$  functional groups after  $K_3PO_4$  modification. A similar conclusion was drawn from the O 1s peaks. In addition, the peak of  $Si-O-P$  ( $245.5\text{ eV}$ ) was also observed, suggesting that the binding of P compounds to the modified material was partly due to the high content of Si.<sup>65</sup> XPS has become a powerful tool for further analyzing the electronic structure and chain structure based on the formation of new peaks and peak shifts. However, the characterization methods discussed above only qualitatively analyze the functional groups. They cannot be applied for quantitative evaluation. Boehm titration is a quantification method that can overcome this drawback; a series of reactions between P-rich CHAR and certain reagents (*i.e.* NaOH,  $NaHCO_3$ , HCl) of known volume and concentration can quantify the corresponding functional groups based on the amount of acid or alkali consumed. Although the accuracy of this method is affected by many operational conditions (*i.e.* titration temperature, titration speed, *etc.*),  $-COOH$ ,  $C=O$ ,  $-OH$  and other basic functional groups can be quantified.<sup>60,66</sup> To better understand the changes in the surface functional groups of P-rich CHAR, a combined qualitative and quantitative analysis is urgently needed.

With pores of various sizes, the microstructure of P-rich CHAR is complex. The SSA of P-rich CHAR can be in the wide range of  $5-1500\text{ m}^2\text{ g}^{-1}$ .<sup>6,41</sup> Some studies have shown that the porosity and SSA of P-rich CHAR are dominated mainly by the heating temperature.<sup>67,68</sup> Owing to the water molecules preserved in the pores of P-rich CHAR, the SSA of P-rich CHAR increases with increasing heating temperature. For example, the SSA of  $H_3PO_4$ -modified biochar derived from pine sawdust improved with increasing co-pyrolysis temperatures. The SSA of the modified biochar was two orders of magnitude greater than that of the pristine biochar prepared at  $350\text{ }^\circ\text{C}$ . The SSA of the modified biochar was 4–5 times greater than that of the pristine biochar prepared at  $500\text{ }^\circ\text{C}$  and  $650\text{ }^\circ\text{C}$ .<sup>41</sup> A large SSA suggests greater adsorption sites on the surface of P-rich CHAR. A surface area analyzer can be used to measure the SSA of the P-rich CHAR *via* the Brunauer–Emmett–Teller (BET) method. The determination of SSA by the gas adsorption method is based on



the adsorption characteristics of the gas (usually  $N_2$ ) on the solid surface. Under a certain pressure, the surface of the test sample (adsorbent) presents reversible physical adsorption of the gas molecule (adsorbent) at ultralow temperatures and a gas adsorption equilibrium is reached. By measuring the equilibrium adsorption amount, the SSA of P-rich CHAR can be calculated *via* a theoretical model.

Most P-rich CHAR materials have well-developed pores and smooth surface structures. The bonding P-containing compounds and groups are distributed on the surface and in the pores of the CHAR. Due to the high magnification ratio, scanning electron microscopy (SEM) can be used to directly observe the sample surface and its structures.<sup>7,69</sup> SEM equipped with energy-dispersive X-ray spectroscopy (EDS) can be used to observe the microstructure and semiquantitatively analyze the elements present in the material.<sup>13</sup> Zhou *et al.*,<sup>21</sup> used SEM to scan banana peel hydrochar before and after  $H_3PO_4$  modification and reported that the pristine hydrochar displayed an irregular morphology, rough surfaces, and a dark brown color. Importantly, a much smaller and darker color product was found after  $H_3PO_4$  modification. These results indicate that  $H_3PO_4$  could enhance the catalytic transformation of feedstock, leading to a high degree of carbonization. In addition, transmission electron microscopy (TEM) can be used to observe the microstructure of the P-rich CHAR. Because the magnification of TEM is much greater than that of SEM, TEM can be used to investigate the ultramicrostructure of P-rich CHAR. In TEM analysis, an accelerated and concentrated electron beam is projected onto a very thin sample. The electrons collide with the atoms in the sample and change direction, resulting in angle scattering. The scattering angle is closely related to the density and thickness of the sample. Therefore, light and dark images can be formed. Moreover, X-ray diffraction (XRD) has been used to analyze the forms of C and P present in P-rich CHAR by measuring the angle and intensity of the X-ray diffraction beams after preparation. Generally, carbon crystallites include graphitized and non-graphitized carbon, and the diffraction peaks of these two categories are narrow and broad, respectively.<sup>3,70</sup>

Notably, the characterization and analysis of P-rich CHAR mainly depend on spectral techniques. Although these techniques are conducive to analyzing the total functional group content of P-rich CHAR, they cannot elucidate the molecular structure of dissolved organic carbon (DOC) at different molecular weight levels. Large amounts of DOC, if present in P-rich CHAR entering the environmental system, are bound to participate in the environmental geochemical processes, which can cause certain adverse environmental effects.<sup>71</sup> Therefore, enough attention should be given to managing the DOC. However, there is little research on the structural composition of DOC at the molecular level. As an emerging separation technology, flow field-flow fractionation (FFF) can quickly and gently perform continuous particle size classification of samples.<sup>72</sup> Combined with fluorescence spectroscopy and other technologies, the structure and composition of DOC after classification should be further explored. Therefore, the spectral properties of DOC at different molecular weights can be

obtained. In addition, the emerging high-resolution mass spectrometry methods, especially Fourier transform ion cyclotron resonance mass spectrometry (FT-ICR-MS), can be used to accurately determine the molecular formulas of the thousands of molecules in DOC solutions.<sup>73</sup>

These characteristic techniques can also be used to explore the mechanism after the application of P-rich CHAR.<sup>74</sup> Gao *et al.*,<sup>13</sup> prepared a P-rich biochar by co-pyrolyzing  $KH_2PO_4$ /Ca( $H_2PO_4$ )<sub>2</sub> and rape straw. After modification, the peaks of  $KPO_3$  were seen in the  $KH_2PO_4$ -modified biochar spectrum, and the peaks of  $Ca_2P_2O_7$  appeared in the  $Ca(H_2PO_4)_2$ -modified biochar spectrum. These two P-rich biochars were used to remediate HM(Pb, Cd, and Cu)-contaminated soils. After soil incubation, these two P-rich biochars were separated from the sample, and their XRD patterns revealed a new peak attributed to  $SiO_2$ . The results suggested that, during incubation, these two P-rich biochars could interact with the soil minerals. Moreover, the peaks of  $KPO_3$  and  $Ca_2P_2O_7$  could not be found after soil incubation. Conversely, new peaks corresponding to  $Pb_5P_4O_{15}$  and  $Pb_5(PO_4)_3Cl$  were observed. The reason might be that the P-containing substances in P-rich biochars interact with the HMs in the soil.

## 6. Environmental application of P-rich CHAR

### 6.1 HM immobilization and soil amelioration

As an emerging soil amendment tool, P-rich CHAR has attracted much attention because of its excellent ability to decrease HM mobility, bioavailability, and toxicity in the soil. The relevant reports are presented in Table 1. Zhao *et al.*,<sup>14</sup> confirmed that, after the co-pyrolysis of a phosphate fertilizer (bone meal, triple superphosphate) and sawdust/switchgrass, the ability of the resultant P-modified biochar to immobilize HMs in the soil was markedly enhanced. Compared with the pristine biochar, the Pb, Cu, and Cd immobilization rates of the bone-meal-modified biochar were increased approximately by 4, 2, and 1 times, respectively. These results could be explained by the presence of  $PO_4^{3-}$  in the P-rich biochar, which can precipitate with the HMs. Additionally, the surface functional groups dramatically improved, leading to improved complexation with HMs. Researchers have also reported that CHAR may be noxious because of the toxins present in the raw materials (*i.e.* activated sludge) used. The level of toxicity differs depending on the preparation conditions.<sup>75</sup> Therefore, the risk of P-rich CHAR derived from different raw materials (or prepared under different conditions) should also be evaluated. Owing to the difference in the physicochemical properties of P-modified CHAR derived from different feedstocks, their capacity to immobilize different target metals is different (Table 1). Consequently, when P-rich CHAR is used to remediate HM-contaminated soil, the raw material should be selected based on the target pollutant.

Fig. 5 shows that the HM immobilization mechanisms of P-rich CHAR in soil b mainly include surface complexation, precipitation, ion exchange, electrostatic attraction, and  $\pi-\pi$



Table 1 The application of P-rich CHAR for heavy metal immobilization in soil

| Preparation conditions                | Feedstock                               | Modifying agents  | Application and dosage   | Response  | References |
|---------------------------------------|---|---|--|---|------------|
| Pyrolysis, anaerobism, 550 °C for 2 h | Corn stalk, bamboo, wood, and rice husk | $K_3PO_4$   | Cd- and Cu-contaminated paddy field soil 3%, 5%, and 10%   | $Cu^{2+}$ and $Cd^{2+}$ bioavailability decreased by about 2–3 times. The P-rich biochars derived from rice husk and cornstalk had higher $Cd^{2+}$ and $Cu^{2+}$ immobilization efficiency than the P-rich biochars prepared from the other two feedstocks   | 10         |
| Pyrolysis, anaerobism 500 °C for 2 h  | Rape straw                              | $KH_2PO_4/Ca(H_2PO_4)_2$  | Pb-, Cd-, and Cu-contaminated silt soil 3%   | The leaching toxicities and the ecological risks of Pb, Cd, and Cu were reduced by forming stable fractions, such as metal-P precipitation, complexation, and $\pi-\pi$ electron-donor–acceptor interactions between these metals and the aromatic moieties of P-rich biochar   | 13         |
| Pyrolysis, anaerobism 500 °C for 2 h  | Pine tree sawdust and switchgrass       | Triple superphosphate and bone meal   | Pb-, Cu-, and Cd-contaminated soil 3%  | The HM stabilization capacity of P-rich biochar was significantly improved by the co-pyrolysis of sawdust/switchgrass and a phosphate fertilizer. The modification also resulted in high carbon retention and the slow release of available P   | 14         |
| Pyrolysis, anaerobism 600 °C for 3 h  | Date palm leaves                        | $KH_2PO_4$  | Cd-, Cu-, Pb-, and Zn-contaminated soil 0.5%, 1%, 3%, and 5%   | Adding P-modified biochar improved the available P content and decreased labile HMs in the soil compared with the control and pristine biochar. In P-modified biochar treatment, HMs were transformed to a more stable fraction. Particularly, the 3% modified biochar treatment was most effective in promoting maize growth and the uptake of P. Besides, total HM extraction by the maize plants was also very small | 15         |
| Pyrolysis, anaerobism 500 °C for 4 h  | Wheat straw                             | $KH_2PO_4$  | Stabilization of Cr, Cu, Pb, and Zn during the anaerobic digestion of swine manure 5%, 10%, 15%, and 20% | The addition of $KH_2PO_4$ -modified biochar reduced the DTPA-extractable concentration of Cr, Cu, Pb, and Zn by forming metal-P precipitates. The ecological risk was also decreased by 2 grades. The 5% and 10% dosages exhibited better immobilization efficiency than the others  | 16         |
| Pyrolysis, anaerobism 650 °C for 2 h  | Pig carcass-derived biochar             | The total P concentration in dead pig bodies was greater than $80\text{ g kg}^{-1}$ | Cd- and Pb-contaminated paddy soil 3%  | The P-rich biochar derived from pig carcasses was more effective in stabilizing Pb than the pristine biochars, especially under the redox condition of less than 0 mV, because of the high ash content and phosphates in this P-rich biochar  | 17         |
| Pyrolysis, anaerobism 700 °C for 2 h  | Bamboo                                  | $KH_2PO_4$ modification and crosslink Mg-Al double-hydroxide composite              | Soil contaminated by uranium mill tailings 0%, 1%, 5%, and 10%   | The P-rich biochar composite presented excellent performance in uranium (U) immobilization in the soil at a dosage of 10%, transforming mobile U into immobilized fractions. Moreover, the column leaching experiment reflected that the cumulative loss and leaching efficiency of U were significantly decreased after treatment with this composite  | 18         |



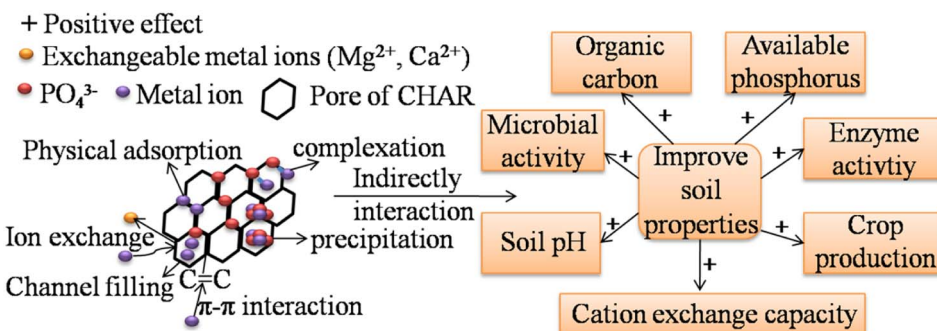


Fig. 5 Remediation mechanisms of HM-contaminated soil by P-modified CHAR and the beneficial effects of P-modified CHAR on soil.

interactions. First, more surface functional groups (*i.e.*  $-\text{COOH}$ ,  $\text{P}=\text{OOH}$ ) are present after modification, which facilitates HM complexation.<sup>13</sup> Secondly, a large number of metal-P precipitates are formed after soil incubation. Thirdly, P-rich CHAR exhibits high aromaticity, for instance, due to the presence of  $\pi$  donors, delivering many  $\pi$  electron clouds into its structure. These  $\pi$  electron clouds can interact with the electron-deficient moieties of HMs and promote HM adsorption.<sup>76</sup> These mechanisms have also been confirmed by the changes in the corresponding FT-IR peak shifts or a decrease before or after incubation.<sup>77</sup> HM immobilization in the soil is also assisted by electrostatic adsorption, channel filling, ion exchange and some basic properties (*i.e.* high SSA value and the microporous and mesoporous structures) of P-rich CHAR. Thus, the overall immobilization of HMs found in the soil is improved.

Owing to the large surface area and high content of C and P, P-rich CHAR has positive effects on soil properties (*i.e.* microbial community structure, soil organic carbon, enzyme activity, and available P content) (Fig. 5).<sup>13,17,24</sup> Among these soil properties, soil organic carbon and available P are critical for HM (Cd, Cu, Pb) immobilization. The application of P-rich CHAR significantly improves the soil organic matter. This organic matter can form metal-organic substances with the HMs in the soil. Besides, adding P-rich CHAR to the soil can transform metal ions into more stable forms, such as metal-P precipitation. Research has shown that adding  $\text{H}_3\text{PO}_4$ -modified banana peel hydrochar increased the cation-exchange capacity, available P, and organic matter in the soil. An improvement in these soil properties results in a decrease in the bioavailability of Cd, Cu and Pb in the soil.<sup>24</sup> Yang *et al.*,<sup>17</sup> confirmed that P-rich biochar was better at immobilizing Pb than pristine biochar, especially under low redox conditions ( $\leq 0$  mV), probably because of the retention of Pb by the phosphates.

## 6.2 Carbon retention

There is increasing concern about climate change caused by greenhouse gas emissions from the soil. The co-pyrolysis/HTC of feedstock and P-containing compounds is an effective way to address this issue because the resultant P-rich CHAR has a high carbon content and captures carbon dioxide emitted by the soil. Typically, the cross-linking reaction of biomass with  $\text{H}_3\text{PO}_4$  intensifies. Cellulose phosphate formation is promoted.

The existence of P-O-C type groups possibly protects the carbon structure, leading to a decrease in carbon loss. Li *et al.*,<sup>19</sup> revealed that, compared with pristine rice straw biochar,  $\text{Ca}(\text{H}_2\text{PO}_4)_2$  modification improved carbon retention by 29%.  $\text{Ca}(\text{H}_2\text{PO}_4)_2$  could facilitate the production of thermally stable phosphorus complexes containing metaphosphates, such as  $\text{C}-\text{PO}_3$  and  $\text{C}-\text{O}-\text{PO}_3$ . These groups prevented carbon decomposition by forming a physical barrier. Thus, the active carbon sites were blocked, and the carbon retention and stability were enhanced.<sup>20</sup>

Zhou *et al.*,<sup>21</sup> used  $\text{H}_3\text{PO}_4$  impregnation-HTC to prepare hydrochar derived from banana peels. When the concentration of  $\text{H}_3\text{PO}_4$  was increased from 0 to 50%, the carbon content in the P-rich hydrochar improved from 63.02 to 89.13%. These results indicate that the hydrochar obtained with a relatively high concentration of  $\text{H}_3\text{PO}_4$  presented a relatively high degree of carbonization. A similar study reported by Zhao *et al.*,<sup>22</sup> revealed that  $\text{H}_3\text{PO}_4$  pretreatment resulted in 70–80% carbon retention in the P-rich biochar derived from pine tree sawdust in contrast to 50% carbon retention without pretreatment. The cross-linking reaction of the P-O-P and C bonds led to more biomass carbon retention in the  $\text{H}_3\text{PO}_4$ -modified biochar. This P-rich biochar had greater Pb adsorption capacity than the unmodified biochar. The main adsorption mechanism was surface physical adsorption and the formation of phosphate precipitates.

Apart from the concentration of the modifying agent, the heating temperature and type of feedstock also strongly influence carbon retention.<sup>20,22</sup> Exploring the influence of preparation conditions and different feedstocks on carbon retention in P-rich CHAR is important. Additionally, the soil components and carbon cycle need to be further investigated with the application of P-rich CHAR.

## 6.3 Slow release of available P

As one of the essential elemental nutrients for plant growth, P commonly accounts for approximately 0.2% of plant dry weight.<sup>78</sup> Owing to the lack and/or partial fixation of available P in the soil, the growth of crops is limited. This barrier causes negative effects on nearly 30% of the farmlands worldwide.<sup>79</sup> Particularly in saline-alkali soil, P deficiency is more severe. Soil salinization is the main factor that restricts food production,

Table 2 The application of P-rich CHAR for heavy metal adsorption in aqueous solutions

| Preparation conditions  | Feedstock                         | Modifying agents  | Heavy metals                          | Response   | References |
|---|-----------------------------------|---|---------------------------------------|--|------------|
| Pyrolysis, anaerobism 500 °C and 2 h                            | Rape straw                        | $\text{Ca}(\text{H}_2\text{PO}_4)_2\text{H}_2\text{O}$ , $\text{KH}_2\text{PO}_4$ | $\text{Pb}^{2+}$                      | The maximum adsorption capacities of $\text{Ca}(\text{H}_2\text{PO}_4)_2\text{H}_2\text{O}$ -modified biochar and $\text{KH}_2\text{PO}_4$ -modified biochar for $\text{Pb}^{2+}$ (566.3 and 1559, $\text{mmol g}^{-1}$ , respectively) were much higher than that of the original biochar (184.1 $\text{mmol g}^{-1}$ ). During the pyrolysis process, the P species underwent thermochemical transformation from orthophosphate to pyrophosphate in $\text{Ca}(\text{H}_2\text{PO}_4)_2\text{H}_2\text{O}$ -modified biochar and from orthophosphate to both metaphosphate and pyrophosphate in $\text{KH}_2\text{PO}_4$ -modified biochar, which helped improve Pb adsorption | 11         |
| Pyrolysis, anaerobism 350 °C, 550 °C, 740 °C and 2 h            | Bamboo                            | $\text{Na}_2\text{HPO}_4$   | $\text{Cd}^{2+}$                      | $\text{Na}_2\text{HPO}_4$ modification improved the surface properties of the biochar. The phosphate compound was also bound to its surface. The adsorption capacity of the P-rich biochar was 202.66 $\text{mg g}^{-1}$ . The $\text{Cd}^{2+}$ removal efficiency increased by 85.78%   | 85         |
| Hydrochar, anaerobism 230 °C for 2 h                            | Fresh banana peels                | $\text{H}_3\text{PO}_4$   | $\text{Pb}^{2+}$                      | Moderate amounts of $\text{H}_3\text{PO}_4$ had a positive influence on the physicochemical properties of the hydrochar, when the dosage of $\text{H}_3\text{PO}_4$ was 30%, the prepared P-rich hydrochar presented the best $\text{Pb}^{2+}$ adsorption capacity (241 $\text{mg g}^{-1}$ )   | 21         |
| Hydrochar, anaerobism 230 °C for 2 h                            | Fresh and dehydrated banana peels | $\text{H}_3\text{PO}_4$   | $\text{Pb}^{2+}$                      | The P-rich hydrochar derived from dehydrated and fresh banana peels presented excellent performance in $\text{Pb}^{2+}$ adsorption. The addition of $\text{H}_3\text{PO}_4$ helped the formation of abundant surface functional groups. Ion exchange was probably the main adsorption mechanism  | 86         |
| Pyrolysis, anaerobism 200 °C, 350 °C, 500 °C and 650 °C for 2 h | Pine sawdust                      | $\text{H}_3\text{PO}_4$   | $\text{Cu}^{2+}$ and $\text{Cd}^{2+}$ | The number of surface functional groups on the P-rich biochars increased compared with that on the pristine biochar at the same pyrolysis temperature, which was conducive to $\text{Cu}^{2+}$ and $\text{Cd}^{2+}$ adsorption. The newly formed P-containing groups ( <i>i.e.</i> $\text{P}=\text{O}$ and $\text{P}=\text{OOH}$ ) could also complex with $\text{Cu}^{2+}$ and $\text{Cd}^{2+}$   | 41         |
| Pyrolysis, anaerobism 450 °C for 1 h                            | Chicken feather                   | $\text{H}_3\text{PO}_4$   | $\text{Cd}^{2+}$ and $\text{Pb}^{2+}$ | The maximum $\text{Cd}^{2+}$ and $\text{Pb}^{2+}$ adsorption capacities of the modified biochar was 1.38 and 5.41 times higher than that of the non-modified biochar, respectively. The main adsorption mechanisms were precipitation, O–H bonding, and electrostatic adsorption   | 60         |
| Hydrochar, in air atmosphere, 250 °C for 2 h                    | Pomelo peel                       | $\text{H}_3\text{PO}_4$   | $\text{Ag}^+$ and $\text{Pb}^{2+}$    | The modified biochar prepared from pomelo peel had high $\text{Ag}^+$ and $\text{Pb}^{2+}$ adsorption capacities (137.4 and 88.7 $\text{mg g}^{-1}$ , respectively). The high-efficiency removal of $\text{Ag}^+$ was the result of its adsorption and reduction to Ag-containing particles. Conversely, $\text{Pb}^{2+}$ was adsorbed and precipitated as $\text{Pb}_5(\text{PO}_4)_3\text{OH}$   | 87         |



Table 2 (Contd.)

| Preparation conditions                                   | Feedstock                             | Modifying agents                | Heavy metals                          | Response   | References |
|--|---------------------------------------|---------------------------------|---------------------------------------|--|------------|
| Hydrochar, in air atmosphere, 120 °C for 2 h             | Cauliflower leaves                    | H <sub>3</sub> PO <sub>4</sub>  | Cu <sup>2+</sup> and Pb <sup>2+</sup> | The P-rich hydrochar prepared from cauliflower leaves contained more -OH and -COOH on its surface than those on the non-modified hydrochar, leading to its excellent performance, with maximum Cu <sup>2+</sup> and Pb <sup>2+</sup> adsorption capacities of 81.43 and 224.60 mg g <sup>-1</sup> , respectively. Moreover, the newly formed P-containing groups, such as P=OOH and P=O, could also enhance adsorption | 8          |
| Pyrolysis, anaerobism 600 °C for 1 h                     | Coffee residue                        | H <sub>3</sub> PO <sub>4</sub>  | Pb <sup>2+</sup> and Cd <sup>2+</sup> | The adsorption capacities of the H <sub>3</sub> PO <sub>4</sub> -modified biochar derived from coffee residue were higher for Pb <sup>2+</sup> and Cd <sup>2+</sup> (89.28 mg g <sup>-1</sup> and 46.95 mg g <sup>-1</sup> ) than those of the ZnCl <sub>2</sub> -modified biochar (63.29 mg g <sup>-1</sup> and 37.04 mg g <sup>-1</sup> , respectively)  | 81         |
| Pyrolysis, anaerobism 350 °C, 500 °C, and 600 °C for 2 h | Pine tree sawdust                     | H <sub>3</sub> PO <sub>4</sub>  | Pb <sup>2+</sup>                      | Compared with the pristine biochar, not only were the basic properties of the H <sub>3</sub> PO <sub>4</sub> -modified biochar improved, but it also presented excellent Pb <sup>2+</sup> adsorption capability. These characteristics are possibly attributed to the precipitation reaction of Pb <sup>2+</sup> with PO <sub>4</sub> <sup>3-</sup>  | 22         |
| Pyrolysis, anaerobism 350 °C for 1 h                     | <i>Taraxacum mongolicum</i> Hand-Mazz | KH <sub>2</sub> PO <sub>4</sub> | As <sup>3+</sup>                      | The presence of P on the surface of the biochar improved the efficiency of As <sup>3+</sup> removal from contaminated water. The adsorption tests presented that the maximum As <sup>3+</sup> adsorption of the P-modified biochar was 30.76 mg g <sup>-1</sup>  | 88         |

food security and land use.<sup>23</sup> Consequently, to meet the long-term requirements of crop growth, P fertilizers are needed. However, the traditional method involves the application of excessive chemical P fertilizers. These chemical fertilizers always depend on P extraction from phosphate rocks, which are nonrenewable. In addition, only 10–15% percent of phosphorus present in the chemical fertilizer can be absorbed by plants, indicating that the utilization rate of P from fertilizers is usually low.<sup>80</sup> The unabsorbed P enters water bodies *via* leaching and surface runoff. The loss of P results in many environmental problems (*i.e.* eutrophication).<sup>23,80</sup> It is critical to explore the use of slow-release fertilizers containing P in the soil. Because of the given existing formation of P in slow-release P fertilizers, these fertilizers can delay P absorption by plants. Another reasonable definition is that, compared with traditional fertilizers that contain rapidly available P (such as potassium dihydrogen phosphate, and ammonium phosphate), the release time of P in slow-release P fertilizers is significantly prolonged. This way, the P utilization rate can be improved, and the long-term P requirement for plant growth is met.<sup>9</sup>

The application of P-rich CHAR is one of the main methods to replace traditional chemical fertilizers and improve available

P levels in the soil.<sup>81</sup> Because the carbonization process can increase the degradation of polyphosphates to orthophosphates, the dominant P component of the CHAR is converted to Fe/Al-bound P. This P fraction is usually considered as a buffer form because Fe/Al-bound P gradually releases soluble P into the soil. For instance, Chu *et al.*,<sup>23</sup> cultured *Chlorella vulgaris* and *Microcystis* sp. in wastewater with high P contents. To recycle P, the collected microalgae were then converted into P-rich hydrochar *via* HTC at 200 °C and 260 °C. The total content of P in the P-rich hydrochar prepared at 260 °C was greater than that in the hydrochar prepared at 200 °C. The comparison suggests that a higher HTC temperature would produce greater P content in the hydrochar. Moreover, increasing the HTC temperature not only increased the total P content in the P-rich hydrochar markedly but also increased the proportions of Fe/Al-bound and Ca-bound P. The proportions of soluble and exchangeable P (both of which are referred to as available P) decreased. With increasing heating temperatures and hydrolysis, the soluble and exchangeable P fractions would decompose. Most soluble substances are dissolved in the reaction system. Due to the mass conservation of Fe, Al and Ca, the mineral-bound P fractions increase in the P-rich CHAR. Fe/Al-



bound P is considered a moderately labile P pool for plants. The P concentration can differ between the P releaser and P adsorbent depending on the environment.<sup>82</sup> Therefore, P-rich CHAR releases available P more slowly and persistently than traditional chemical P fertilizers. Zhao *et al.*<sup>14</sup> drew a similar conclusion based on a P-rich biochar synthesized by the co-pyrolysis of sawdust and triple superphosphate/bone meal. Its adsorption kinetics indicated that the rate constant of P release (0.0012–0.0024) was much lower than that of the pristine biochar (0.012). The equilibrium experiment suggested that the rate constant for P-rich biochar (0.89–0.91) presented a similar trend to that of pristine biochar (1.79). These studies provide a promising strategy for improving the P utilization efficiency by plants. Besides, it has been shown that the solubility ( $K_{SP-Fe} = 9.9 \times 10^{-16}$  and  $K_{SP-Al} = 5.8 \times 10^{-19}$ ) of the  $Fe^{3+}$  and  $Al^{3+}$  precipitates with  $PO_4^{3-}$  is greater than that ( $K_{SP-Ca} = 2.0 \times 10^{-29}$ ) of the  $Ca^{2+}$  precipitate.<sup>83,84</sup> Although most P is converted to Fe/Al-bound P, a small portion of Ca-bound P and residual P remains in the P-rich CHAR. As they act as buffer forms of available P in weathered soils, these two P fractions should be given more focus in the future and taken full advantage of. Further studies should focus on changing the P release behavior of P-rich CHAR.

#### 6.4 HM removal from wastewater

P-rich CHAR is known to be good at adsorbing HMs (*i.e.*  $Zn^{2+}$ ,  $Cu^{2+}$ ,  $Cd^{2+}$ ,  $Pb^{2+}$ ) in aqueous solutions (Table 2). The serious harm caused by these inorganic pollutants to the environment, animals, and human health can be alleviated by P-rich CHAR. Fig. 6 summarizes the HM adsorption mechanisms and the preparation strategies of P-rich CHAR. Owing to the high surface area and the release of soluble P compounds (*i.e.*  $HPO_4^{2-}$ ,  $PO_4^{3-}$ ) into the solution, a series of physicochemical reactions, such as surface adsorption, complexation, metal-P precipitation and ion exchange, can take place.<sup>18,81</sup> To accurately regulate P-rich CHAR at the molecular level in the future, a quantitative description of these adsorption mechanisms is necessary.

Many factors (*i.e.* the preparation conditions, the type and dosage of the modifying agent, the type of pristine biomass, and the concentration of HMs) affect the HM adsorption capacity of

P-rich CHAR. With regard to modifying agents, the P content and chemical characteristics of these agents dominate the adsorption capacity of P-rich CHAR. For example,  $H_3PO_4$ -modified CHAR shows remarkably enhanced HM adsorption in wastewater.<sup>89,90</sup> CHAR modified with other inorganic P-containing compounds (*i.e.*  $Na_2HPO_4$ ,  $KH_2PO_4$ , and  $Ca(H_2PO_4)_2$ ) have also been shown to improve HM adsorption.<sup>11,85</sup> In addition, modification conditions (*i.e.* temperature and redox potential), such as chain length, solubility, and crystallinity, affect the properties of the polyphosphates. These properties predominantly improve the ability to precipitate and (or) complex with metals. In addition, surface mineral elements (*i.e.* Ca and Mg) present on the P-rich CHAR might probably affect the HM adsorption capacity. Further investigations regarding the influence of these factors on the HM adsorption performance of P-rich CHAR are needed.

## 7. Problems and challenges

Due to the outstanding performance in HM adsorption and immobilization, carbon retention and the slow release of available P, P-rich CHAR has garnered significant attention over the past decade. However, given the inherent complexity and variability of the environmental systems, their potential negative impacts should not be overlooked.

(1) Limited scale of P-rich CHAR production: the production of P-rich CHAR remains confined to the experimental scale, largely due to its limited application at a larger scale. On the one hand, the influence of the preparation parameters on the adsorption and immobilization of HMs, slow release of available P, and C retention by P-rich CHAR remains unclear. Previous works have focused mainly on the factors influencing pristine CHAR production. On the other hand, as the scale-up of P-rich CHAR production progresses, minimizing production costs becomes critical, posing a risk of potential trade-off between quantity and quality. Although the HTC method is more energy-efficient, the wastewater generated during HTC requires treatment, and additional solid-liquid operation is inevitable.

(2) Need for novel synthesis methods: different preparation methods impact the fundamental properties of P-rich CHAR. The development of new synthesis techniques may yield P-rich CHAR with unique physical or chemical characteristics that enhance its pollutant removal potential.

(3) Specificity of pollutant removal: P-rich CHAR derived from a particular feedstock under certain conditions may have a high capacity for adsorption and (or) immobilization of specific HMs. Moreover, it can exhibit poor performance for other pollutants. For instance, although the  $K_3PO_4$ -modified biochar derived from rice husk had a high efficiency of Cd and Cu immobilization in the soil, the extraction and mobility for arsenic increased.<sup>10</sup>

Because water/soil environments contaminated with HMs are complicated, there is a lack of comprehensive evaluation of the eco-environmental risks posed by P-rich CHAR.

(4) Laboratory-scale research and economic considerations: most studies done on the application of P-rich CHAR are still at

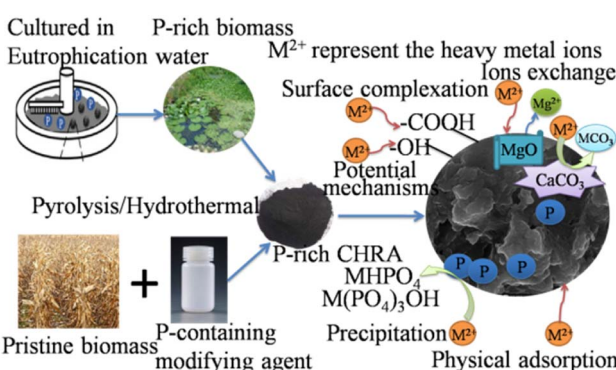


Fig. 6 Summary of the preparation strategies of P-modified CHAR and its HM adsorption mechanisms.



the laboratory scale. Considering the high cost of P sources, it is challenging to accurately evaluate the P utilization efficiency. Moreover, the potential toxic effects of P-rich CHAR, such as the release of polycyclic aromatic hydrocarbons, raise concerns about its environmental aging. The long-term effects of P-rich CHAR remain largely unexplored.

(5) Knowledge gaps regarding dissolved organic carbon (DOC): given the potential of large-scale application of P-rich CHAR as an additive in the soil and water, dissolved organic carbon (DOC) from P-rich CHAR may enter the environment and interact with various geochemical processes. Current studies predominantly focus on DOC from natural soils and water bodies, whereas studies on DOC derived from P-rich CHAR are limited. This creates a knowledge gap in the understanding of DOC in the natural environment and DOC from P-rich CHAR.

(6) Potential for eutrophication: while P-rich CHAR shows excellent performance in terms of HM adsorption in water, it may also release excessive P into aquatic systems, leading to eutrophication. Moreover, despite the high HM immobilization capacity of P-rich CHAR for certain pollutants found in contaminated soil, P loss through leaching and runoff is a potential concern. Future research should aim to enhance metal removal efficiency while mitigating eutrophication in water and P loss in the soil. Two possible solutions are as follows: (1) for specific soil types, the optimum application dosage of P-rich CHAR should be explored. This can be realized by response surface optimization or single factor optimization. (2) Attempts should be made to completely separate P-rich CHAR from water or soil after application by processing it into a granular form or magnetizing it. These approaches cannot only improve the adsorption efficiency of HMs found in water (or the immobilization rate of HMs in the soil) but also enhance the separation of P-rich CHAR from water/soil.

(7) Challenges related to slow release of P: although P-rich CHAR possesses a certain capacity for slow release of P, its P release rate remains faster than what is typically required for plant growth. The utilization rate of phosphorus fertilizer is generally low, meaning that only a fraction of the applied phosphorus is absorbed by plants. This rapid release may not meet the long-term P demands of plants.

(8) Lack of quality standards and production guidelines: P-rich CHAR production lacks standard quality criteria. Current production technologies do not adhere to uniform guidelines, such as permissible concentrations of toxic elements in raw materials, minimum carbonization temperatures, retention times and post-carbonization treatment. The establishment of comprehensive production and application standards for P-rich CHAR is urgently needed.

## 8. Future research directions

In light of the challenges discussed above, future research on P-rich CHAR remains essential across various fields. The prospective research directions are summarized as follows:

(1) Exploration of unconventional preparation methods: greater attention should be given to unconventional

preparation techniques, such as secondary pyrolysis and ball milling combined with thermochemical methods. Comprehensive investigations of the preparation parameters are necessary to optimize the P doping ratio and improve the characteristics of P-rich CHAR.

(2) Focus on pollutant interactions: future research should prioritize studying the interactions between P-rich CHAR, soil/water environments, and specific pollutants to better understand the mechanisms governing pollutant adsorption, immobilization, and removal.

(3) Influence of raw materials and preparation conditions: the influence of various factors, such as the source of raw materials and preparation conditions, on the yield and physicochemical properties of the resultant P-rich CHAR materials requires further exploration. Additionally, the mechanisms underlying P-rich CHAR preparation and the regulation of key active components need to be thoroughly investigated.

(4) Long-term field application: future studies should focus on the long-term (more than two years) field application of P-rich CHAR at a large scale. To reduce costs, natural P-rich waste should be utilized as raw material.

(5) Environmental behavior of the DOC: the environmental behavior and molecular composition of DOC derived from P-rich CHAR should receive more attention, particularly in the context of its interactions with soil and water systems.

(6) Assessment of environmental risks: before the large-scale application of P-rich CHAR, environmental risks associated with excess P in water and soil need to be thoroughly evaluated to prevent potential adverse effects, such as eutrophication.

(7) Enhancement of the phosphorus release efficiency: future research should aim to improve the slow-release capacity of available P in P-rich CHAR into the soil and increase the efficiency of P utilization to meet plant nutrient requirements over longer periods.

(8) Life cycle assessment and database development: a comprehensive life cycle assessment of P-rich CHAR needs to be established. The database should include raw material, production, processing details and application. The creation of a dedicated database will provide valuable scientific data to support the future application of P-rich CHAR in various environmental and agricultural settings.

## 9. Conclusion

This review presents the research advancements in the field of P-rich CHAR, offering insights from the studies on P-modified and P-laden CHAR published in the past decade. An overall picture of the preparation, characterization, environmental application and existing challenges of P-rich CHAR is provided in detail. Unlike pristine or other modified CHAR, P-rich CHAR possesses distinct properties, such as elevated C and P contents and abundant P-containing functional groups. These properties facilitate carbon retention, slow release of available P, and the adsorption and immobilization of HMs in water and soil. In addition to physical adsorption, mechanisms, such as ion exchange, surface complexation and precipitation, further elucidate their improved pollutant removal capability.



Moreover, enhanced characterization technologies are essential to explain the molecular structure of P-rich CHAR. The environmental risks associated with its application warrant further assessment, along with a comprehensive evaluation of the risks linked to its large-scale use. In summary, P-rich CHAR presents an environmentally friendly, effective and viable solution for organic solid waste management and environmental remediation.

## Data availability

No primary research results, software or code have been included, and no new data were generated or analyzed as part of this review.

## Author contributions

Qilong Ge: investigation, methodology, data curation, writing – original draft. Chunjuan Dong: conceptualization, methodology, software, data curation, writing – reviewing & editing, supervision, validation. Guoqing Wang: supervision, project administration. Jing Zhang: writing – reviewing & editing, visualization. Rui Hou: resources, data curation, investigation, software.

## Conflicts of interest

There are no conflicts to declare.

## Acknowledgements

This work was jointly supported by the Basic Research Programs of Shanxi Province, China (No. 202303021222225 and No. 202103021223009).

## Notes and references

- 1 R. Sharma, K. Jasrotia, N. Singh, P. Ghosh, S. Srivastava, N. R. Sharma, J. Singh, R. Kanwar and A. Kumar, A comprehensive review on hydrothermal carbonization of biomass and its applications, *Chem. Afr.*, 2020, **3**, 1–19.
- 2 M. Sharma, J. Singh, C. Baskar and A. Kumar, A comprehensive review on biochar formation and its utilization for wastewater treatment, *Pollut. Res.*, 2018, **37**, S1–S18.
- 3 J. Wang and S. Wang, Preparation, modification and environmental application of biochar: a review, *J. Cleaner Prod.*, 2019, **227**, 1002–1022.
- 4 X. R. Jing, Y. Y. Wang, W. J. Liu, Y. K. Wang and H. Jiang, Enhanced adsorption performance of tetracycline in aqueous solutions by methanol-modified biochar, *Chem. Eng. J.*, 2014, **248**, 168–174.
- 5 P. Zhang, S. Liu, X. Tan, Y. Liu, G. Zeng, Z. Yin, S. Ye and Z. Zeng, Microwave-assisted chemical modification method for surface regulation of biochar and its application for estrogen removal, *Process Saf. Environ. Prot.*, 2019, **128**, 329–341.
- 6 P. Netherway, S. M. Reichman, M. Laidlaw, K. Scheckel, N. Pingitore, G. Gascó, A. Méndez, A. Surapaneni and J. Paz-Ferreiro, Phosphorus-rich biochars can transform lead in an urban contaminated soil, *J. Environ. Qual.*, 2019, **48**, 1091–1099.
- 7 L. Pei, F. Yang, X. Xu, H. Nan, X. Gui, L. Zhao and X. Cao, Further reuse of phosphorus-laden biochar for lead sorption from aqueous solution: isotherm, kinetics, and mechanism, *Sci. Total Environ.*, 2021, **792**, 148550.
- 8 Q. Ge, Q. Tian, M. Moeen and S. Wang, Facile synthesis of cauliflower leaves biochar at low temperature in the air atmosphere for Cu(II) and Pb(II) removal from water, *Materials*, 2020, **13**, 3163.
- 9 B. S. D. Onishi, C. S. dos Reis Ferreira, A. Urbano and M. J. Santos, Modified hydrotalcite for phosphorus slow-release: kinetic and sorption-desorption processes in clayey and sandy soils from North of Paraná state (Brazil), *Appl. Clay Sci.*, 2020, **197**, 105759.
- 10 H. Zhang, J. Shao, S. Zhang, X. Zhang and H. Chen, Effect of phosphorus-modified biochars on immobilization of Cu(II), Cd(II), and As(V) in paddy soil, *J. Hazard. Mater.*, 2020, 121349.
- 11 R. Gao, Q. Fu, H. Hu, Q. Wang, Y. Liu and J. Zhu, Highly-effective removal of Pb by co-pyrolysis biochar derived from rape straw and orthophosphate, *J. Hazard. Mater.*, 2019, **371**, 191–197.
- 12 X. An, Z. Wu, X. Liu, W. Shi, F. Tian and B. Yu, A new class of biochar-based slow-release phosphorus fertilizers with high water retention based on integrated co-pyrolysis and copolymerization, *Chemosphere*, 2021, **285**, 131481.
- 13 R. Gao, H. Hu, Q. Fu, Z. Li, Z. Xing, U. Ali, J. Zhu and Y. Liu, Remediation of Pb, Cd, and Cu contaminated soil by co-pyrolysis biochar derived from rape straw and orthophosphate: speciation transformation, risk evaluation and mechanism inquiry, *Sci. Total Environ.*, 2020, **730**, 139119.
- 14 L. Zhao, X. Cao, W. Zheng, J. W. Scott, B. K. Sharma and X. Chen, Copyrolysis of biomass with phosphate fertilizers to improve biochar carbon retention, slow nutrient release, and stabilize heavy metals in soil, *ACS Sustain. Chem. Eng.*, 2016, **4**, 1630–1636.
- 15 M. Ahmad, A. R. A. Usman, A. S. Al-Faraj, M. Ahmad, A. Sallam and M. I. Al-Wabel, Phosphorus-loaded biochar changes soil heavy metals availability and uptake potential of maize (*Zea mays* L.) plants, *Chemosphere*, 2018, **194**, 327–339.
- 16 S. Yang, Q. Wen and Z. Chen, Effect of KH<sub>2</sub>PO<sub>4</sub>-modified biochar on immobilization of Cr, Cu, Pb, Zn and As during anaerobic digestion of swine manure, *Bioresour. Technol.*, 2021, **339**, 125570.
- 17 X. Yang, H. Pan, S. M. Shaheen, H. Wang and J. Rinklebe, Immobilization of cadmium and lead using phosphorus-rich animal-derived and iron-modified plant-derived biochars under dynamic redox conditions in a paddy soil, *Environ. Int.*, 2021, **156**, 106628.
- 18 P. Lyu, G. Wang, Y. Cao, B. Wang and N. Deng, Phosphorus-modified biochar cross-linked Mg-Al layered double-



hydroxide composite for immobilizing uranium in mining contaminated soil, *Chemosphere*, 2021, **276**, 130116.

19 F. Li, X. Cao, L. Zhao, J. Wang and Z. Ding, Effects of mineral additives on biochar formation: carbon retention, stability, and properties, *Environ. Sci. Technol.*, 2014, **48**, 11211–11217.

20 F. Li, X. Gui, W. Ji and C. Zhou, Effect of calcium dihydrogen phosphate addition on carbon retention and stability of biochars derived from cellulose, hemicellulose, and lignin, *Chemosphere*, 2020, **251**, 126335.

21 N. Zhou, H. Chen, Q. Feng, D. Yao, H. Chen, H. Wang, Z. Zhou, H. Li, Y. Tian and X. Lu, Effect of phosphoric acid on the surface properties and Pb(II) adsorption mechanisms of hydrochars prepared from fresh banana peels, *J. Cleaner Prod.*, 2017, **165**, 221–230.

22 L. Zhao, W. Zheng, O. Mašek, X. Chen, B. Gu, B. K. Sharma and X. Cao, Roles of phosphoric acid in biochar formation: synchronously improving carbon retention and sorption capacity, *J. Environ. Qual.*, 2017, **46**, 393–401.

23 Q. Chu, T. Lyn, L. Xue, L. Yang, Y. Feng, Z. Sha, B. Yue, R. J. G. Mortimer, M. Cooper and G. Pan, Hydrothermal carbonization of microalgae for phosphorus recycling from wastewater to crop-soil systems as slow-release fertilizers, *J. Cleaner Prod.*, 2021, **283**, 124627.

24 Q. Ge, Q. Tian, R. Hou and S. Wang, Combing phosphorus-modified hydrochar and zeolite prepared from coal gangue for highly effective immobilization of heavy metals in coal-mining contaminated soil, *Chemosphere*, 2022, **291**, 132835.

25 M. Xu, P. Gao, Z. Yang, L. Su, J. Wu, G. Yang, X. Zhang, J. Ma, H. Peng and Y. Xiao, Biochar impacts on phosphorus cycling in rice ecosystem, *Chemosphere*, 2019, **225**, 311–319.

26 S. Marathe and L. Sadowski, Developments in biochar incorporated geopolymers and alkali activated materials: a systematic literature review, *J. Cleaner Prod.*, 2024, **469**, 143136.

27 M. Wang, Y. Zhu, L. Cheng, B. Andserson, X. Zhao, D. Wang and A. Ding, Review on utilization of biochar for metal-contaminated soil and sediment remediation, *J. Environ. Sci.*, 2018, **63**, 156–173.

28 M. Ahmad, A. U. Rajapaksha, J. E. Lim, M. Zhang, N. Bolan, D. Mohan, M. Vithanage, S. S. Lee and Y. S. Ok, Biochar as a sorbent for contaminant management in soil and water: a review, *Chemosphere*, 2014, **99**, 19–33.

29 J. Jin, M. Kang, K. Sun, Z. Pan, F. Wu and B. Xing, Properties of biochar amended soils and their sorption of imidacloprid, isoproturon, and atrazine, *Sci. Total Environ.*, 2016, **550**, 504–513.

30 M. Wilk and A. Magdziarz, Hydrothermal carbonization, torrefaction and slow pyrolysis of *Miscanthus giganteus*, *Energy*, 2017, **140**, 1292–1304.

31 Y. C. Wang, J. J. Ni, H. W. Guo and E. Kravchenko, Influences of phosphorus-modified biochar on bacterial community and diversity in rhizosphere soil, *Environ. Sci. Pollut. Res.*, 2024, **31**, 1681–1691.

32 W. W. Ng, Y. C. Wang, J. J. Ni and P. S. So, Effects of phosphorus-modified biochar as a soil amendment on the growth and quality of *Pseudostellaria heterophylla*, *Sci. Rep.*, 2022, **12**(1), 7268.

33 G. Kumar, S. Shobana, W. H. Chen, Q. V. Bach, S. H. Kim, A. E. Atabani and J. S. Chang, A review of thermochemical conversion of microalgal biomass for biofuels: chemistry and processes, *Green Chem.*, 2016, **19**, 44–67.

34 D. Daer, L. Luo, Y. W. Shang, J. X. Wang, C. Z. Wu and Z. G. Liu, Co-hydrothermal carbonization of waste biomass and phosphate rock: promoted carbon sequestration and enhanced phosphorus bioavailability, *Biochar*, 2024, **6**, 70.

35 P. Yuan, J. Wang, Y. Pan, B. Shen and C. Wu, Review of biochar for the management of contaminated soil: preparation, application and prospect, *Sci. Total Environ.*, 2019, **659**, 473–490.

36 A. Méndez, S. Barriga, F. Guerrero and G. Gascó, Thermal analysis of growing media obtained from mixtures of paper mill waste materials and sewage sludge, *J. Therm. Anal. Calorim.*, 2011, **104**, 213–221.

37 Z. Guo, X. Bian, J. Zhang, H. Liu, C. Cheng, C. Zhang and J. Wang, Activated carbons with well-developed microporosity prepared from *Phragmites australis* by potassium silicate activation, *J. Taiwan Inst. Chem. Eng.*, 2014, **45**, 2801–2804.

38 E. Cárdenas-Aguilar, G. Gascó, J. Paz-Ferreiro and A. Méndez, The effect of biochar and compost from urban organic waste on plant biomass and properties of an artificially copper polluted soil, *Int. Biodeterior. Biodegrad.*, 2017, **124**, 223–232.

39 B. L. Chen and Z. M. Chen, Sorption of naphthalene and 1-naphthol by biochars of orange peels with different pyrolytic temperatures, *Chemosphere*, 2009, **76**, 127–133.

40 H. Zhang, W. Liao, X. Zhou, J. Shao, Y. Chen, S. Zhang and H. Chen, Coeffect of pyrolysis temperature and potassium phosphate impregnation on characteristics, stability, and adsorption mechanism of phosphorus-enriched biochar, *Bioresour. Technol.*, 2022, **344**, 126273.

41 H. Peng, P. Gao, G. Chu, B. Pan, J. Peng and B. Xing, Enhanced adsorption of Cu(II) and Cd(II) by phosphoric acid-modified biochars, *Environ. Pollut.*, 2017, **229**, 846–853.

42 X. Dai, N. T. H. Nhung, M. E. Hamza, Y. X. Guo, L. Chen, C. L. He, S. Ning, Y. Wei, G. Dodbiba and T. Fujita, Selective adsorption and recovery of scandium from red mud leachate by using phosphoric acid pre-treated pitaya peel biochar, *Sep. Purif. Technol.*, 2022, **292**, 121043.

43 Q. Ge, Q. Tian, K. Feng, S. Wang and R. Hou, Effects of co-application of phosphorus-modified hydrochar and zeolite on the release of soil available phosphorus, *Environ. Sci. Res.*, 2022, **35**(1), 219–229, DOI: [10.13198/j.issn.1001-6929.2021.08.27](https://doi.org/10.13198/j.issn.1001-6929.2021.08.27), in Chinese.

44 S. Y. Foong, R. K. Liew, Y. Yand, Y. W. Chen, P. N. Yuh Yek, W. A. W. Mahari, X. Y. Lee, C. S. Han, D. V. Vo, Q. V. Le, M. Aghbashlo, M. Tabatabaei, C. Sonne, W. Peng and S. S. Lam, Valorization of biomass waste to engineered activated biochar by microwave pyrolysis: progress, challenges, and future directions, *Chem. Eng. J.*, 2020, **389**, 124401.

45 S. Nizamuddin, H. A. Baloch, G. J. Griffin, N. M. Mubarak, A. W. Bhutto, R. Abro, S. A. Mazari and B. S. Ali, An overview of effect of process parameters on hydrothermal



carbonization of biomass, *Renewable Sustainable Energy Rev.*, 2017, **73**, 1289–1299.

46 W. Buss, M. C. Graham, J. G. Shepherd and O. Masek, Suitability of marginal biomass-derived biochars for soil amendment, *Sci. Total Environ.*, 2016, **547**, 314–322.

47 Y. Yi, Z. Huang, B. Lu, J. Xian, E. P. Tsang, W. Cheng, J. Fang and Z. Fang, Magnetic biochar for environmental remediation: a review, *Bioresour. Technol.*, 2020, **298**, 122468.

48 H. A. H. I. Amarasinghe, S. K. Gunathilake and A. K. Karunaratne, Ascertaining of optimum pyrolysis conditions in producing refuse tea biochar as a soil amendment, *Procedia Food Sci.*, 2016, **6**, 97–102.

49 A. Janus, A. Pelfrene, S. Heymans, C. Deboffe, F. Douay and C. Waterlot, Elaboration, characteristics and advantages of biochars for the management of contaminated soils with a specific overview on *Miscanthus* biochars, *J. Environ. Manage.*, 2015, **162**, 275–289.

50 Saifullah, S. Dahlawi, A. Naeem, Z. Rengel and R. Naidu, Biochar application for the remediation of salt-affected soils: challenges and opportunities, *Sci. Total Environ.*, 2018, **625**, 320–335.

51 J. D. Aparicio, C. S. Benimeli, C. A. Almeida, M. A. Polti and V. L. Colin, Integral use of sugarcane vinasse for biomass production of actinobacteria: potential application in soil remediation, *Chemosphere*, 2017, **181**, 478–484.

52 K. L. Yu, B. F. Lau, P. L. Show, H. C. Ong, T. C. Ling, W. H. Chen, E. P. Ng and J. S. Chang, Recent developments on algal biochar production and characterization, *Bioresour. Technol.*, 2017, **246**, 2–11.

53 C. Torri, C. Samorì, A. Adamiano, D. Fabbri, C. Faraloni and G. Torzillo, Preliminary investigation on the production of fuels and biochar from *Chlamydomonas reinhardtii* biomass residue after bio-hydrogen production, *Bioresour. Technol.*, 2011, **102**, 8707–8713.

54 Q. Wang, C. J. Duan, C. Y. Xu and Z. C. Geng, Efficient removal of Cd(II) by phosphate-modified biochars derived from apple tree branches: processes, mechanisms, and application, *Sci. Total Environ.*, 2022, **819**, 152876.

55 A. Hussain, Z. Zhang, Z. Guo, R. Li, A. Mahar, M. Kumar, P. Wang, F. Shen, F. Kumbhar, T. Ali, J. Zhao and D. Guo, Beneficial effects of tobacco biochar combined with mineral additives on (im)mobilization and (bio)availability of Pb, Cd, Cu and Zn from Pb/Zn smelter contaminated soils, *Ecotoxicol. Environ. Saf.*, 2017, **145**, 528–538.

56 C. Tan, Z. Zeyu, H. Rong, M. Ruihong, W. Hongtao and L. Wenjing, Adsorption of cadmium by biochar derived from municipal sewage sludge: impact factors and adsorption mechanism, *Chemosphere*, 2015, **134**, 286–293.

57 H. S. Kambo and A. Dutta, A comparative review of biochar and hydrochar in terms of production, physico-chemical properties and applications, *Renewable Sustainable Energy Rev.*, 2015, **45**, 359–378.

58 Z. Wang, X. Yang, T. Qin, G. Liang, Y. Li and X. Xie, Efficient removal of oxytetracycline from aqueous solution by a novel magnetic clay-biochar composite using natural attapulgite and cauliflower leaves, *Environ. Sci. Pollut. Res.*, 2019, **26**, 7463–7475.

59 H. Q. Luo, Y. K. Zhang, Y. Xie, Y. Li, M. Qi, R. Ma, S. Yang and Y. Wang, Iron-rich microorganism-enabled synthesis of magnetic biocarbon for efficient adsorption of diclofenac from aqueous solution, *Bioresour. Technol.*, 2019, **282**, 310–317.

60 H. Chen, W. Li, J. Wang, H. Xu, Y. Liu, Z. Zhang, Y. Li and Y. Zhang, Adsorption of cadmium and lead ions by phosphoric acid-modified biochar generated from chicken feather: selective adsorption and influence of dissolved organic matter, *Bioresour. Technol.*, 2019, **292**, 121948.

61 Y. Xue, B. Gao, Y. Yao, M. Inyang, M. Zhang, A. R. Zimmerman and K. S. Ro, Hydrogen peroxide modification enhances the ability of biochar (hydrochar) produced from hydrothermal carbonization of peanut hull to remove aqueous heavy metals: batch and column tests, *Chem. Eng. J.*, 2012, **200–202**, 673–680.

62 S. Ying, R. Keey, Y. Yang, Y. Wang, P. Nai, Y. Yek, W. Adibah, W. Mahari, X. Yi, C. Sean and D. N. Vo, Valorization of biomass waste to engineered activated biochar by microwave pyrolysis: progress, challenges, and future directions, *Chem. Eng. J.*, 2020, **389**, 124401.

63 C. Zhang, L. Zhang, J. Gao, S. Zhang, Q. Liu, P. Duan and X. Hu, Evolution of the functional groups/structures of biochar and heteroatoms during the pyrolysis of seaweed, *Algal Res.*, 2020, **48**, 101900.

64 J. Dai and Y. S. Liu, Review of research on the properties of biochar and its applications in soil, *Chin. J. Soil Sci.*, 2013, **44**, 1520–1525.

65 W. Zhang, X. Li and R. Yang, Study on the change of silicon and phosphorus content in the condensed phase during the combustion of epoxy resin with OPS/DOPO, *Polym. Degrad. Stab.*, 2014, **99**, 298–303.

66 H. P. Boehm, Some aspects of the surface chemistry of carbon blacks and other carbons, *Carbon*, 1994, **32**, 759–769.

67 J. W. Lee, M. Kidder, B. R. Evans, S. Paik, C. T. Garten and R. C. Brown, Characterization of biochars produced from cornstovers for soil amendment, *Environ. Sci. Technol.*, 2010, **44**, 7970–7974.

68 J. Chen, D. Fang and F. Duan, Pore characteristics and fractal properties of biochar obtained from the pyrolysis of coarse wood in a fluidized-bed reactor, *Appl. Energy*, 2018, **218**, 54–65.

69 Y. Hamid, L. Tang, B. Hussain, M. Usman, H. Kumar, M. Saqib, Z. He and X. Yang, Efficiency of lime, biochar, Fe containing biochar and composite amendments for Cd and Pb immobilization in a co-contaminated alluvial soil, *Environ. Pollut.*, 2020, **257**, 113609.

70 S. Yoo, S. Kelley, D. Tilotta and S. Park, Structural characterization of loblolly pine derived biochar by X-ray diffraction and electron energy loss spectroscopy, *ACS Sustain. Chem. Eng.*, 2018, **6**, 2621–2629.

71 J. Jin, K. Sun, Z. Wang, Y. Yang, L. Han and B. Xing, Characterization and phenanthrene sorption of natural and pyrogenic organic matter fractions, *Environ. Sci. Technol.*, 2017, **51**, 2635–2642.



72 H. Xu, H. Lin, H. Jiang and L. Guo, Dynamic molecular size transformation of aquatic colloidal organic matter as a function of pH and cations, *Water Res.*, 2018, **144**, 543–552.

73 B. P. Koch, M. Witt, R. Engbrodt, T. Dittmar and G. Kattner, Molecular formulae of marine and terrigenous dissolved organic matter detected by electrospray ionization Fourier transform ion cyclotron resonance mass spectrometry, *Geochim. Cosmochim. Acta*, 2005, **69**, 3299–3308.

74 X. Cao, L. Ma, B. Gao and W. Harris, Dairy-manure derived biochar effectively sorbs lead and atrazine, *Environ. Sci. Technol.*, 2009, **43**, 3285–3291.

75 S. Kong, X. Yao, J. Zhang, X. Yao and H. Zeng, Review of characteristics of biochar and research progress of its application, *Ecol. Environ. Sci.*, 2015, **24**, 716–723.

76 G. Song, Y. Guo, G. Li, W. Zhao and Y. Yu, Comparison for adsorption of tetracycline and cefradine using biochar derived from seaweed *Sargassum* sp., *Desalin. Water Treat.*, 2019, **160**, 316–324.

77 H. N. Tran, S. J. You and H. P. Chao, Fast and efficient adsorption of methylene green 5 on activated carbon prepared from new chemical activation method, *J. Environ. Manage.*, 2017, **188**, 322–336.

78 M. J. Adegbeye, P. Ravi Kanth Reddy, A. I. Obaisi, M. M. M. Y. Elghandour, K. J. Oyebamiji, A. Z. M. Salem, O. T. Morakinyo-Fasipe, M. Cipriano-Salazar and L. M. Camacho-Díaz, Sustainable agriculture options for production, greenhouse gasses and pollution alleviation, and nutrient recycling in emerging and transitional nations - an overview, *J. Cleaner Prod.*, 2020, **242**, 118329.

79 B. Li, T. Yin, I. A. Udagama, S. L. Dong, W. Yu, Y. F. Huang and B. Young, Food waste and the embedded phosphorus footprint in China, *J. Cleaner Prod.*, 2020, **252**, 119909.

80 J. Tian, X. R. Wang, Y. P. Tong, X. P. Chen and H. Liao, Bioengineering and management for efficient phosphorus utilization in crops and pastures, *Curr. Opin. Biotechnol.*, 2012, **23**, 866–871.

81 J. A. Kim, K. Vijayaraghavan, D. H. K. Reddy and Y. S. Yun, A phosphorus-enriched biochar fertilizer from bio-fermentation waste: a potential alternative source for phosphorus fertilizers, *J. Cleaner Prod.*, 2018, **196**, 163–171.

82 Y. H. Fei, D. Zhao, Y. D. Cao, H. Huot, Y. T. Tang, H. Zhang and T. Xiao, Phosphorous retention and release by sludge-derived hydrochar for potential use as a soil amendment, *J. Environ. Qual.*, 2019, **48**, 502–509.

83 L. Dai, F. Tan, B. Wu, M. He, W. Wang, X. Tang, Q. Hu and M. Zhang, Immobilization of phosphorus in cow manure during hydrothermal carbonization, *J. Environ. Manage.*, 2015, **157**, 49–53.

84 X. Cui, M. Lu, M. B. Khan, C. Lai, X. Yang, Z. He, G. Chen and B. Yan, Hydrothermal carbonization of different wetland biomass wastes: phosphorus reclamation and hydrochar production, *Waste Manage.*, 2020, **102**, 106–113.

85 S. Zhang, H. Zhang, J. Cai, X. Zhang, J. Zhang and J. Shao, Evaluation and prediction of cadmium removal from aqueous solution by phosphate-modified activated bamboo biochar, *Energy Fuels*, 2018, **32**, 4469–4477.

86 N. Zhou, H. Chen, J. Xi, D. Yao, Z. Zhou, Y. Tian and X. Lu, Biochars with excellent Pb(II) adsorption property produced from fresh and dehydrated banana peels via hydrothermal carbonization, *Bioresour. Technol.*, 2017, **232**, 204–210.

87 T. Zhao, Y. Yao, D. Li, F. Wu, C. Zhang and B. Gao, Facile low-temperature one-step synthesis of pomelo peel biochar under air atmosphere and its adsorption behaviors for Ag(I) and Pb(II), *Sci. Total Environ.*, 2018, **640**–641, 73–79.

88 W. Ahmed, S. Mehmood, A. Núñez-Delgado, S. Ali, M. Qaswar, A. Shakoor, A. A. Maitlo and D. Y. Chen, Adsorption of arsenic(III) from aqueous solution by a novel phosphorus-modified biochar obtained from *Taraxacum mongolicum* Hand-Mazz: adsorption behavior and mechanistic analysis, *J. Environ. Manage.*, 2021, **292**, 11276.

89 Y. Huang, S. Li, J. Chen, X. Zhang and Y. Chen, Adsorption of Pb(II) on mesoporous activated carbons fabricated from water hyacinth using  $H_3PO_4$  activation: adsorption capacity, kinetic and isotherm studies, *Appl. Surf. Sci.*, 2014, **293**, 160–168.

90 Q. Jiang, W. Xie, S. Han, Y. Wang and Y. Zhang, Enhanced adsorption of Pb(II) onto modified hydrochar by polyethyleneimine or  $H_3PO_4$ : an analysis of surface property and interface mechanism, *Colloids Surf. A*, 2019, **583**, 123962.

